

Supporting Information

Crumpled and porous N-doped MXene microspheres for promoting sulfur redox kinetics in Li–S batteries

Xiaolu Yu et. al

Experimental Section

Chemicals and materials: Ti_3AlC_2 (500 mesh) was purchased from Laizhou Kai Kai Ceramic Materials Co., Ltd., China. Diethylenetriamine solvent (99.0%) was bought from Shanghai Macklin Biochemical Technology Co., Ltd., China. Sulfur powders (99.5%) were purchased from Shanghai Guangnuo Chemical Technology Co., Ltd., China.

Preparation of N–MXene and MXene: First, the aqueous $\text{Ti}_3\text{C}_2\text{T}_x$ MXene solution (2 mg mL^{-1}) was fabricated by a classical acid etching and subsequent manual exfoliation strategy.¹ Then 50 mL diethylenetriamine solvent was mixed uniformly with 25 mL MXene solution by constant stirring for 30 min. Afterwards, the mixture was treated in the reaction kettle under 180 °C for 12 h. After cooling, the resultant products were washed with deionized water by centrifugation to remove any residual impurities. Finally, the N–MXene was obtained after freeze drying. MXene was fabricated by directly freeze drying the aqueous $\text{Ti}_3\text{C}_2\text{T}_x$ MXene solution.

Preparation of S cathode: To fabricate the S cathode, super-P and S powders were mixed with a mass ratio of 3:7 to obtain a uniform mixture. Then the mixture was heated for 12 h in an Ar atmosphere, forming the S/C composite. Afterwards, S/C composite was mixed with super-P and polyvinylidenefluoride (PVDF) with a mass ratio of 7:2:1. The formed mixture was dispersed in N-methylpyrrolidinone (NMP) solution to form a uniform slurry, which was coated on a piece of carbon coated Al foil. After drying for 12 h at 60 °C in vacuum, the S cathode was obtained. The S electrode used in coin batteries was 1 cm in diameter. The mass loading of active S on cathode was 1.1 mg cm^{-2} .

Preparation of modified separators: The MXene or N–MXene modified separator was prepared through a wet coating strategy. First, MXene or N–MXene was mixed with PVDF with

a mass ratio of 9:1 to form a uniform mixture. The mixture was then uniformly dispersed in NMP to form a homogeneous slurry, which was then coated on one surface of separator (Celgard2325) followed by a drying process in vacuum at 40 °C for 12 h. Finally, the modified separators were cut into discs with a diameter of 16 mm. The mass loading of MXene or N–MXene on separator was 0.1 mg cm⁻².

Preparation of MXene or N–MXene modified Cu: First, MXene or N–MXene was mixed with PVDF (9:1 in mass ratio) to form a mixture. Then the mixture was dispersed in NMP to form a uniform slurry. The slurry was coated on Cu foil. After drying in vacuum at 60 °C for 12 h, the modified Cu was achieved. The modified Cu electrode used in coin batteries was 1.2 cm in diameter.

Samples characterization: X-ray diffraction (XRD, MiniFlex 600, Japan) was utilized to investigate the phase compositions of samples. X-ray photoelectron spectrometer (XPS, Axis Supra, Japan) was used to probe the surface properties of samples. The structure of samples was probed by scanning electron microscope field-emission transmission electron microscopy (TEM, TALOS F200X, USA) and (SEM, JSM-7610F, Japan). Energy dispersive spectrometer (X-max, England) was utilized to probe the distribution of elements on samples. The pore properties of samples were investigated by a fully automatic specific surface area and porosity analyzer (Micromeritics ASAP 2460, USA).

Density functional theory (DFT) calculations: All calculations were performed with the Vienna ab initio Simulation Package (VASP) within the frame of DFT. The details could be found in a previous report.²

Electrochemical measurements: To study the electrochemical performance of samples, 2032-type coin batteries were assembled in an Ar-filled glove box (O₂<0.01 ppm, H₂O<0.01

ppm). The charge-discharge performance of batteries was controlled by a Neware battery test system (CT-4008, Shenzhen, China). The liquid electrolyte in this study was 1 M LiTFSI in 1,3-dioxolane/1,2-dimethoxyethane (DOL/DME, 1:1 by volume) with 1 wt% LiNO₃.

The charge-discharge performance of Li–S batteries was tested between 1.7–2.8 V at various rates (1 C=1675 mA g⁻¹). 20 μ L electrolyte was used in each battery. The Li electrode used in coin batteries was 1.4 cm in diameter. Cyclic voltammetry (CV) of Li–S batteries was tested in 1.7–2.8 V at 0.1 mV s⁻¹.

Kinetic evaluation of polysulfide redox was proceed in a symmetrical battery with two same electrodes by a CV test. The electrode was prepared by coating a mixed slurry of MXene (or N–MXene) and PVDF (9:1 in mass ratio) in NMP on a piece of carbon-coated Al foil followed by a vacuum drying process at 60 °C for 12 h. The diameter of electrode was 1 cm. The electrolyte in symmetrical batteries was 0.2 M Li₂S₆ in LiTFSI-based electrolyte (1 M LiTFSI-DOL/DME, 1:1 by volume with 1 wt% LiNO₃). 40 μ L electrolyte was used in each battery. The CV of symmetrical batteries was tested at 0.5 mV s⁻¹ between -1 and 1 V.

To test the Li plating/stripping Coulombic efficiency (CE) on modified Cu, batteries with modified Cu electrode (1.2 cm in diameter) and Li electrode (1 cm in diameter) were assembled. 40 μ L electrolyte was used in each battery. The batteries were first cycled at 0.05 mA between 0–1 V for 10 cycles to stabilize the interface. Then the batteries were discharged (plating process) for 1 h at 1 mA cm⁻². Subsequently, the batteries were charged (stripping process) to 1 V at 1 mA cm⁻². The CE was the ratio of charging capacity and discharging capacity. To test the cycling and rate performances of symmetrical batteries, 20 mAh cm⁻² of Li was first deposited on modified Cu at 1 mA cm⁻². Then the batteries were cycled at various capacities and current densities.

Composite Li metal anodes used in symmetrical batteries and full batteries were prepared by an electrochemical method at 1 mA cm^{-2} . Modified Cu electrode (1.2 cm in diameter) and Li electrode (1 cm in diameter) were used in the preparation process. Symmetrical batteries with two same composite Li metal anodes were assembled to probe the cycling stability. The batteries were cycled at different current densities and capacities. 40 μL electrolyte was used in each battery. Li–S full batteries with composite Li metal anodes were tested between 1.7–2.8 V at 2 C. The capacity ratio of cathode and anode was controlled to be 1:2.

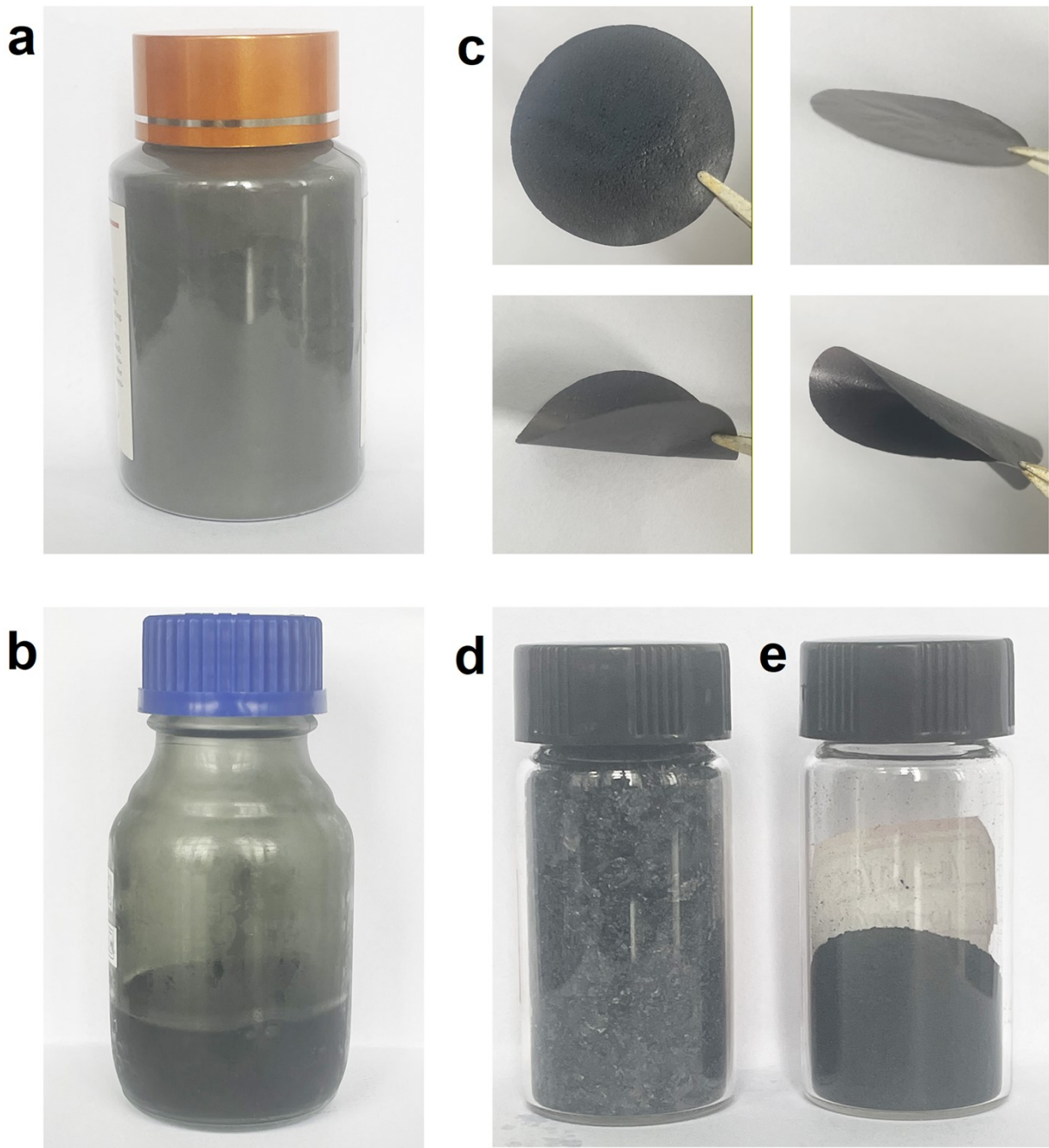


Fig. S1 (a) Photograph of a bottle of Ti_3AlC_2 powders. (b) Photograph of a bottle of aqueous $\text{Ti}_3\text{C}_2\text{T}_x$ solution. (c) Photographs of MXene films. (d) Photograph of a bottle of freeze-dried MXene. (e) Photograph of a bottle of N-MXene.

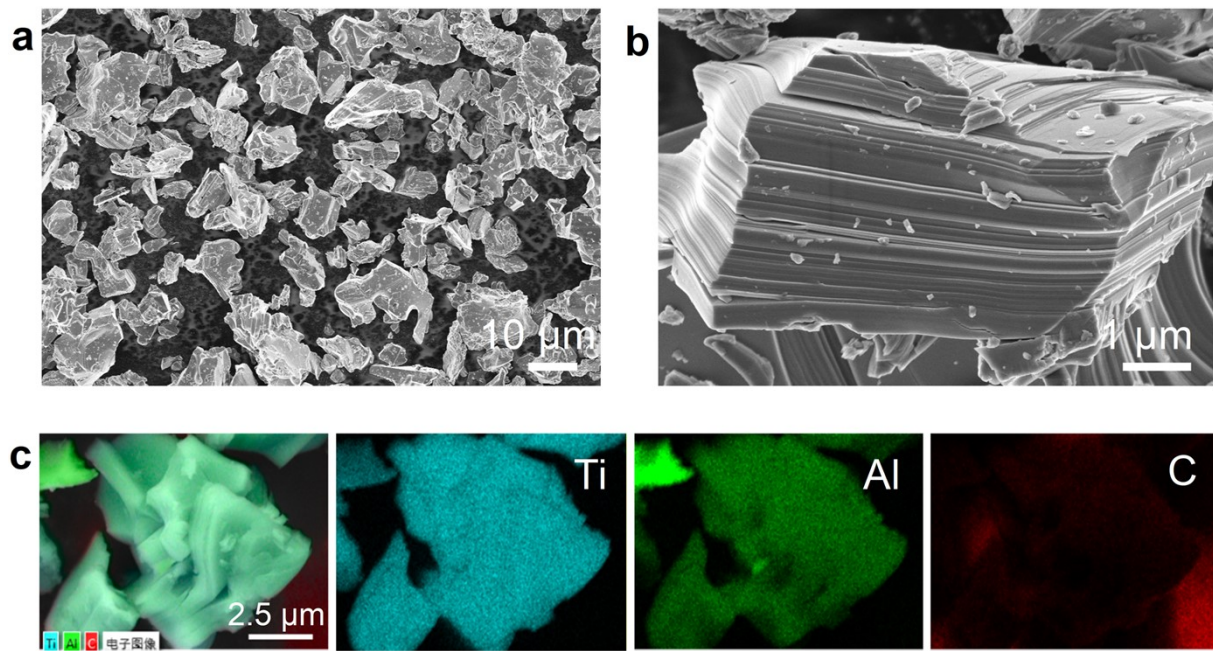


Fig. S2 (a,b) SEM images of Ti_3AlC_2 powders. (c) SEM image of Ti_3AlC_2 powders and corresponding EDS mapping.

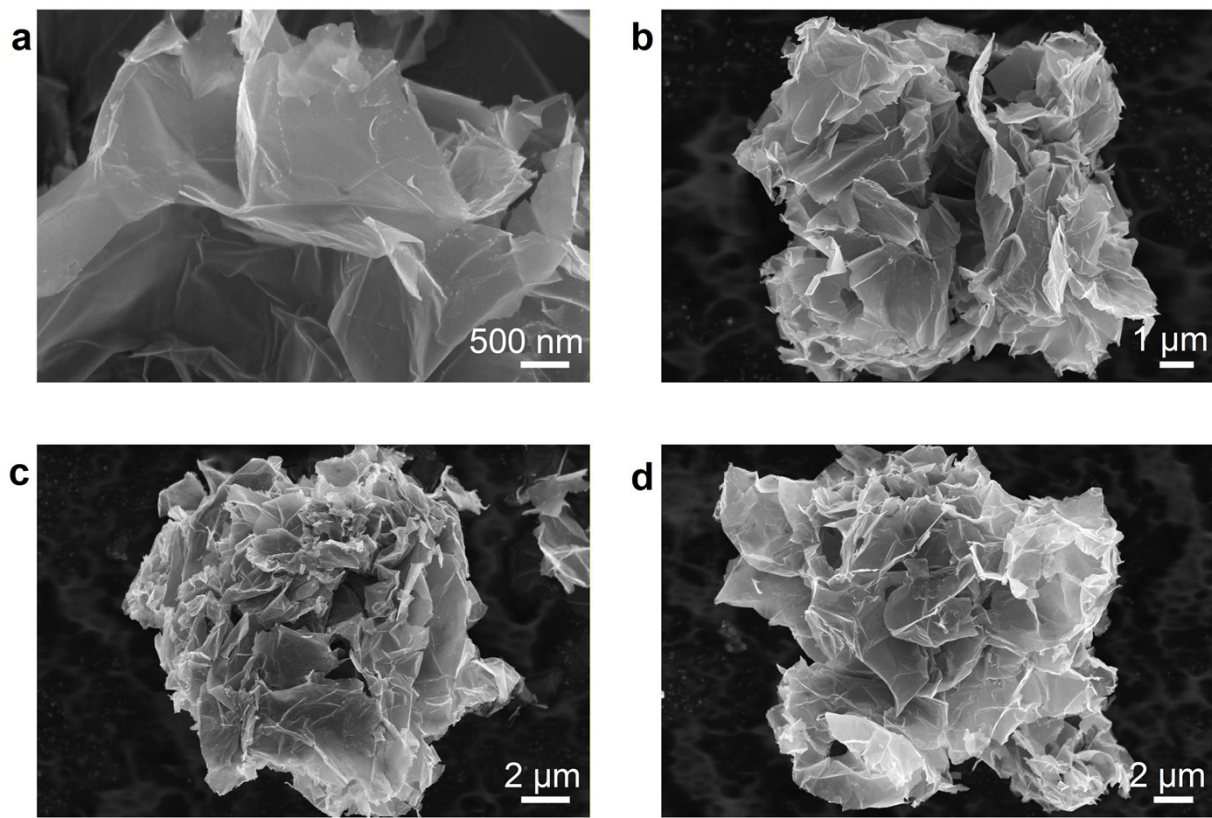


Fig. S3 (a–d) SEM images of N–MXene.

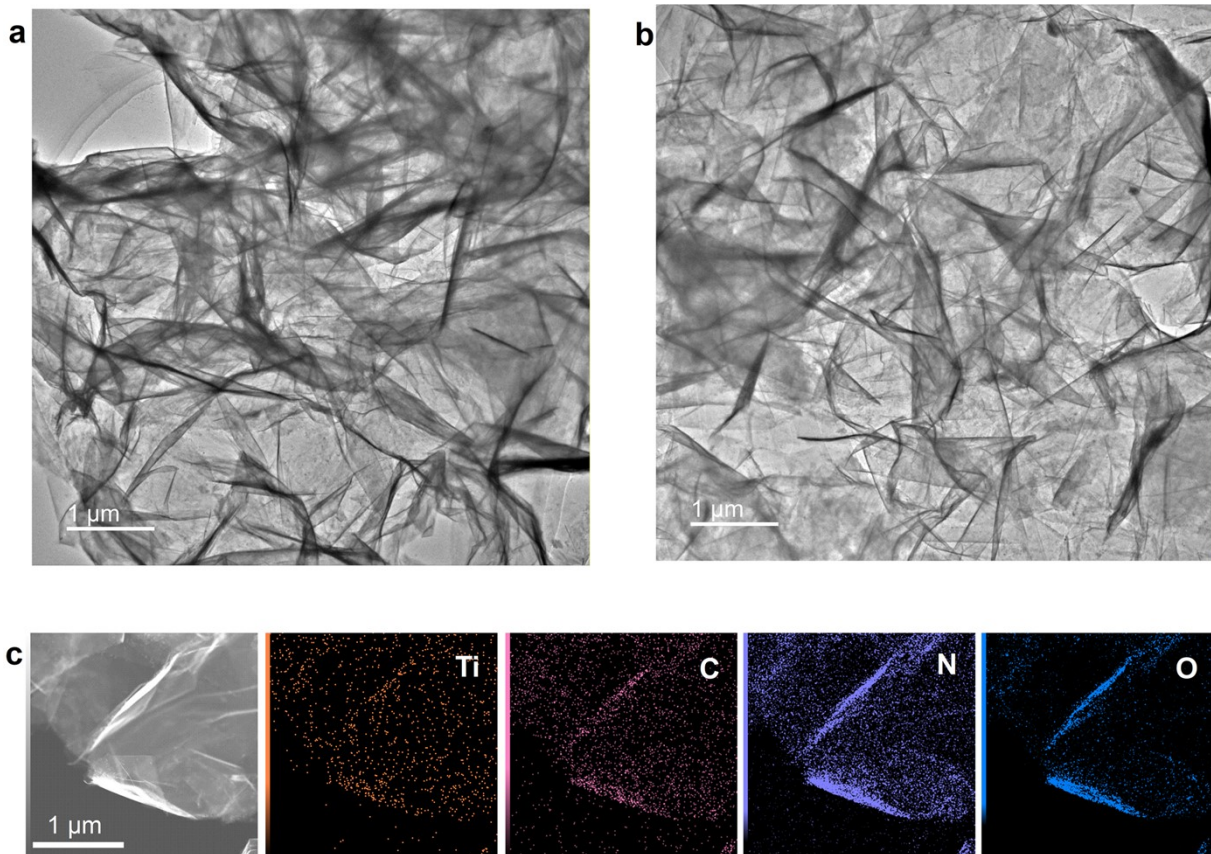


Fig. S4 (a,b) TEM images of N–MXene. (c) TEM image of N–MXene and corresponding EDS mapping.

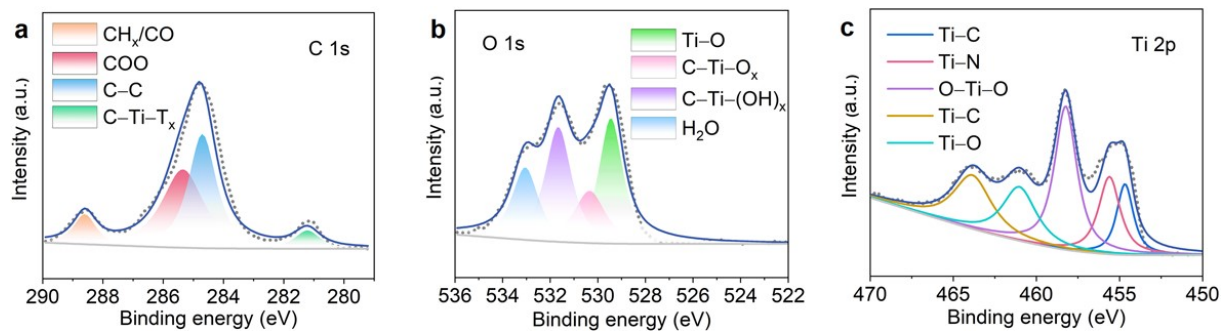


Fig. S5 (a–c) High-resolution XPS spectra of C 1s, O 1s, and Ti 2p in N–MXene, respectively.

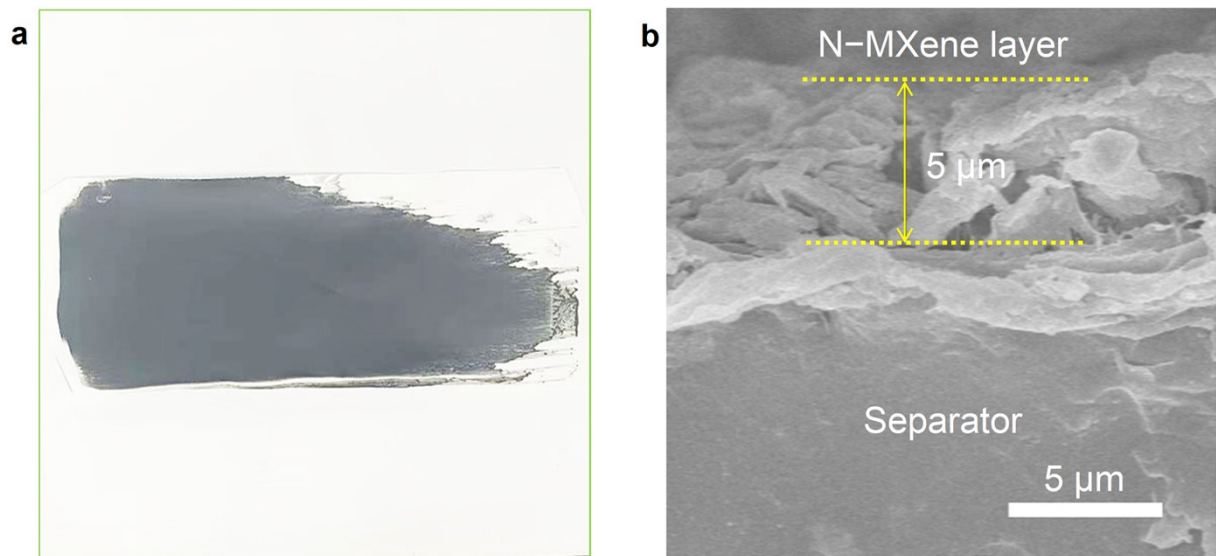


Fig. S6 (a) A photograph of N-MXene modified separator. (b) Cross-sectional SEM image of N-MXene modified separator.

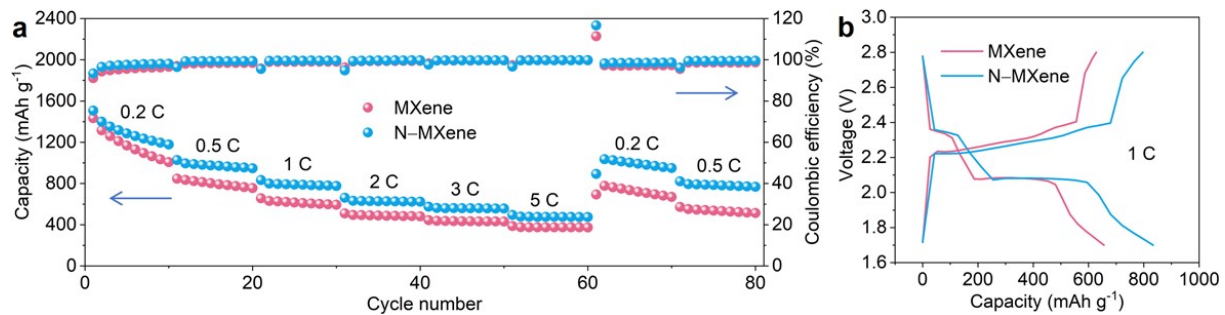


Fig. S7 (a) Rate performance of Li–S batteries with different separators. (b) Charge-discharge curves of Li–S batteries with different separators at 1 C.

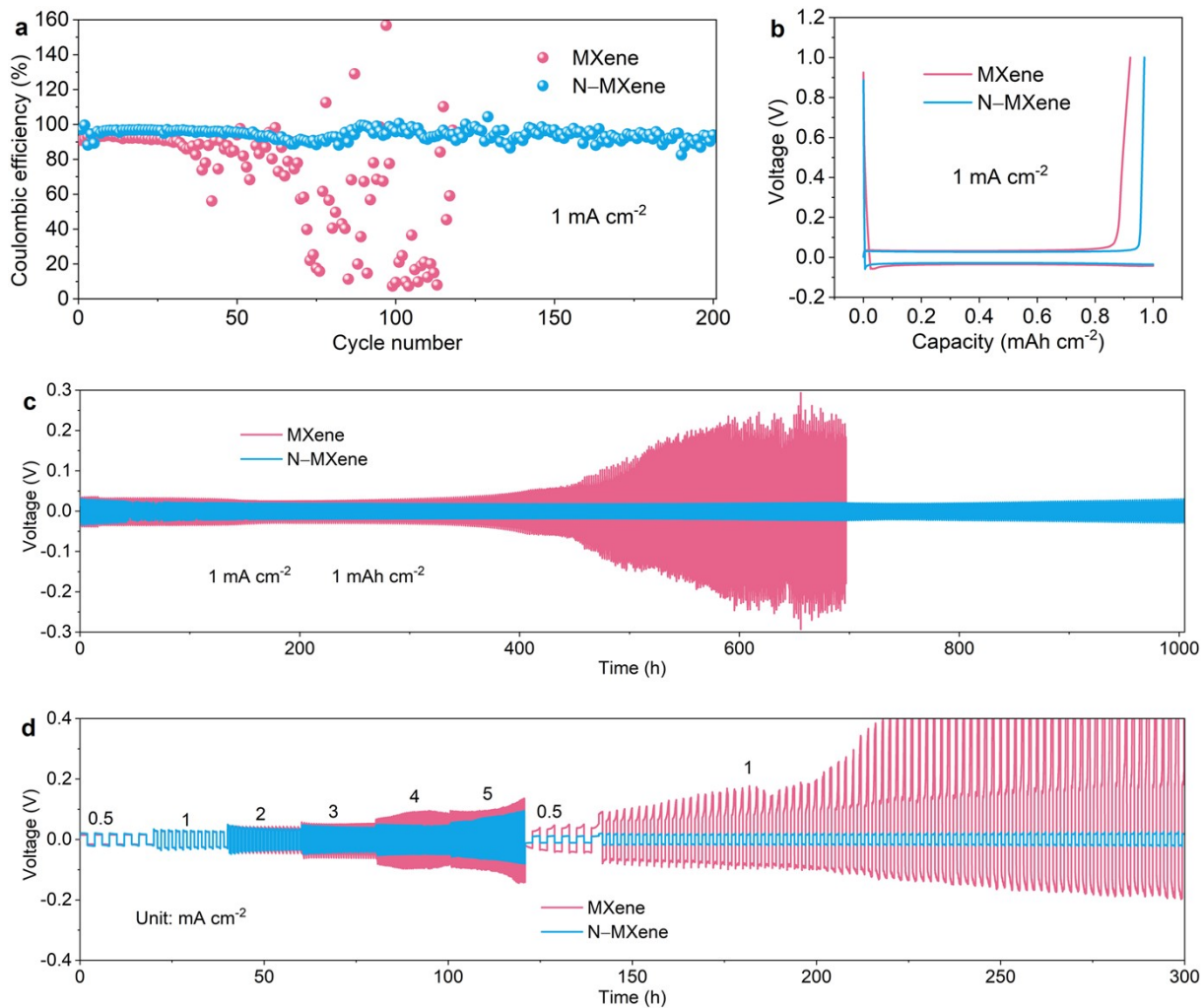


Fig. S8 (a) CE and (b) Li plating/stripping curves of MXene and N-MXene. (c) Cycling performance of different composite Li metal anodes at 1 mA cm^{-2} . (d) Rate performance of symmetrical battery at various current densities with different composite Li metal anodes (limited capacity: 1 mAh cm^{-2}).

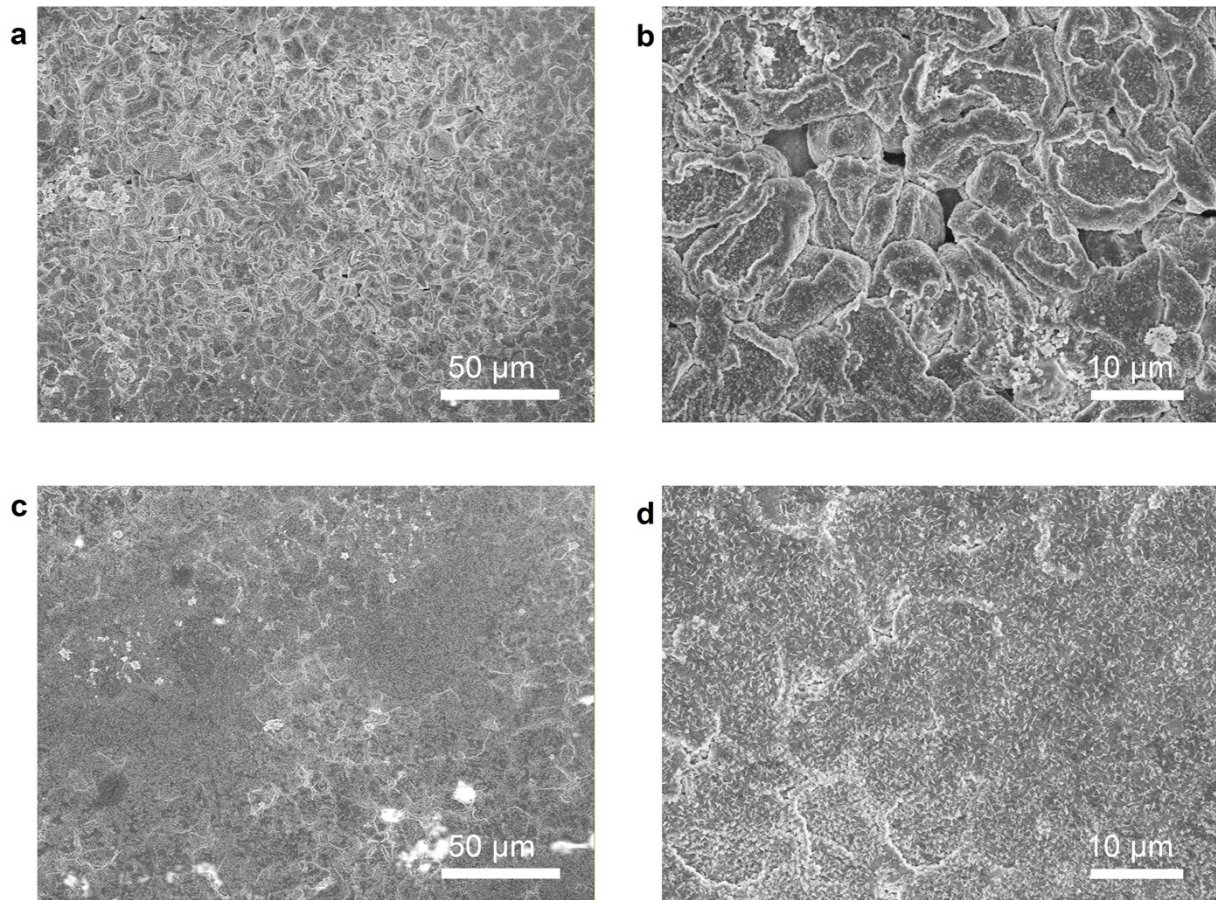


Fig. S9 (a,b) SEM images after plating 5 mAh cm⁻² of Li on MXene modified Cu at 1 mA cm⁻². (c,d) SEM images after plating 5 mAh cm⁻² of Li on N-MXene modified Cu at 1 mA cm⁻².

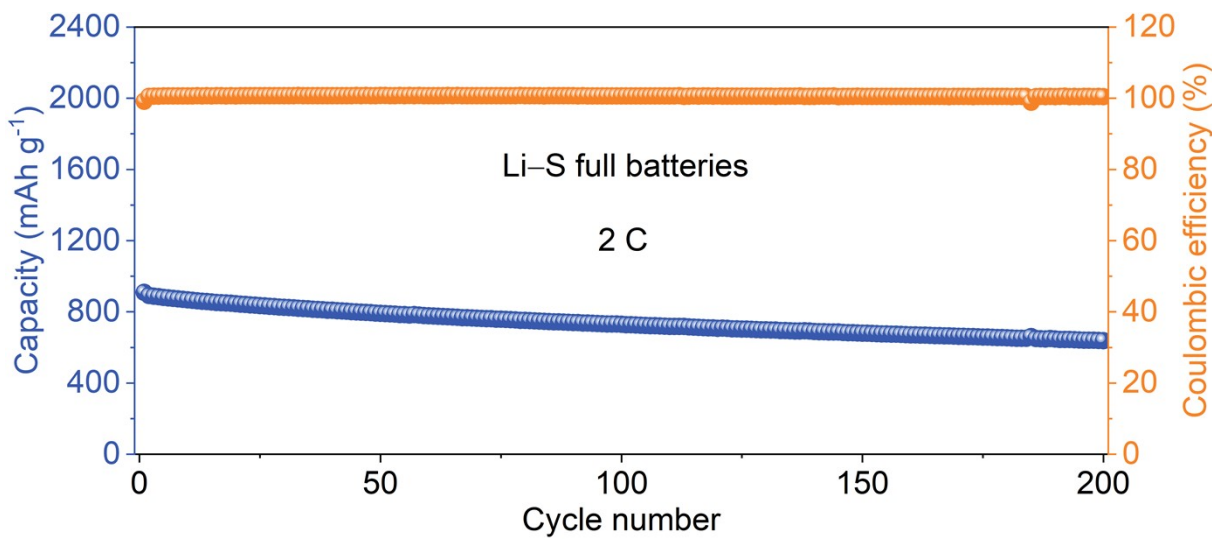


Fig. S10 Cycling performance of Li-S full batteries with N-MXene modified separator and N-MXene based composite Li metal anode at 2 C.

Note: N-MXene was also investigated as a host for Li metal anode to address its interface issues. Coulombic efficiency (CE) test showed N-MXene enabled a higher Li plating/stripping CE than MXene (Fig. S8a). The better CE of N-MXene was attributed to its porous structure and abundant lithiophilic active sites (surface groups and doped N).³ The porous structure could relieve the volume changes of electrode. The lithiophilic active sites could promote uniform Li deposition.^{4,5} In contrast, due to few pores and limited lithiophilic active sites resulted from serious stacking, the CE of MXene was poor. Typical plating/stripping curves further proved lower polarization and higher Li plating/stripping reversibility of N-MXene (Fig. S8b). Long-cycling symmetrical batteries revealed that N-MXene could not only lower the polarization of Li metal anode but also improve its stability compared with MXene. Symmetrical batteries with N-MXene could work for over 1000 h at 1 mA cm⁻² (Fig. S8c). While MXene-based symmetrical batteries failed after only 400 h. Symmetrical batteries with N-MXene host

also showed a better rate capability, especially at high current densities (Fig. S8d). SEM images indicated that the deposited Li on MXene was uneven and dendritic (Fig. S9). Differently, the deposited Li on N–MXene was dense and uniform. So, N–MXene could promote uniform Li deposition due to its porous structure and abundant lithiophilic active sites.

Li–S full batteries with N–MXene modified separator and N–MXene-based composite Li metal anode were assembled to probe the application potential of the strategy proposed in this research. The capacity ratio of cathode and anode in Li–S full batteries was controlled to be 1:2. It could be seen that N–MXene could enable a stable cycling performance of Li–S full batteries at 2 C (Fig. S10). After 200 cycles, a capacity of 638.2 mAh g^{−1} could be retained. This result proved the application ability of N–MXene in practical Li–S batteries.

References

- [1] C. Wei, H. Fei, Y. An, Y. Zhang and J. Feng, *Electrochim. Acta*, 2019, **309**, 362–370.
- [2] C. Wei, Z. Wang, P. Wang, X. Zhang, X. An, J. Feng, B. Xi and S. Xiong, *Sci. Bull.*, 2024, **69**, 2059–2070.
- [3] Y. Fang, Y. Zhang, K. Zhu, R. Lian, Y. Gao, J. Yin, K. Ye, K. Cheng, J. Yan, G. Wang, Y. Wei and D. Cao, *ACS Nano*, 2019, **13**, 14319–14328.
- [4] Z. Wang, Z. Du, Y. Liu, C. E. Knapp, Y. Dai, J. Li, W. Zhang, R. Chen, F. Guo, W. Zong, X. Gao, J. Zhu, C. Wei and G. He, *eScience*, 2024, **4**, 100189.
- [5] H. Liu, C. Wei, Z. Song, Y. Wu, D. Wang, A. Zhou and J. Li, *Chem. Commun.*, 2025, **61**, 5986–5989.